RSC Advances

ROYAL SOCIETY OF CHEMISTRY

www.rsc.org/advances

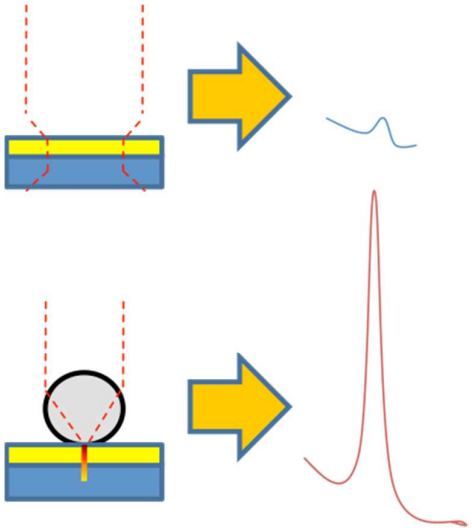

Colloidal lenses can be easily implemented into conventional microspectroscopy experiments as universal, disposable Raman scattering enhancers.

TOC Keyword- Colloidal micro-lenses

Ivano Alessandri,* Nicolò Bontempi, Laura E. Depero

RSC Advances

RSCPublishing

ARTICLE

Colloidal Lenses as Universal Raman Scattering Enhancers

Cite this: DOI: 10.1039/x0xx00000x

I. Alessandri,[a*] N. Bontempi[a] and L. E. Depero[a]

Received ooth,
Accepted oo[th],

DOI: 10.1039/x0xx00000x

www.rsc.org/

SiO_2 microspheres were tested as micro-lenses in a series of Raman experiments, in order to evaluate their potential application in analysis of thin films and molecular species. We demonstrate that colloidal lenses can play as versatile, universal Raman scattering enhancers, that can be easily implemented into conventional microspectroscopy experiments. Our results indicate that colloidal lenses can strongly enhance Raman scattering of all the analytes under investigation, extending their detection limits by several orders of magnitude. Colloidal lenses can be exploited as non-destructive, disposable tools for Raman detection of ultra-thin films. They can also be coupled to either metal- or all-oxide-based SERS active substrates to further boost Raman sensitivity, offering exciting perspectives for ultrasensitive detection and in-situ monitoring of chemical and biochemical reactions under real-working conditions.

Introduction

Colloidal micro-lenses (μ-lenses) can be used to focus, collect and manipulate light at the nanoscale. In 2004 Backman and co-workers demonstrated that sub-wavelength photonic beams ("nanojets") can emerge from the shadow-side of a dielectric microsphere irradiated by a light source of wavelength $\lambda < \varphi$, where φ is the colloidal sphere size.[1] Photonic nanojets are non-evanescent and non-resonant beams (they are generated by a wide range of sphere size) that are characterized by a narrow lateral size (□λ/3) and can propagate over a distance longer than λ, provided that the refractive index contrast between sphere and background is less than 2:1. As a consequence of light concentration, the intensity of the optical field in the focal region can be several orders of magnitude larger than the intensity of the optical source.[2,3] Several applications have been envisioned such as sub-diffraction resolution nanopatterning, ultra high-density optical data storage, optical trapping, waveguiding etc...[3] From the analytical viewpoint this effect have been mainly applied for nanoparticle imaging[4] and two-photon fluorescence.[5] When a dielectric microsphere is irradiated by a focused Gaussian beam the resulting nanojet can be squeezed within a subwavelength dimension not only in transversal but also in longitudinal direction. This three-dimensional confinement of light has been exploited to enhance the fluorescence of single molecules[6-8] or immunocomplexes,[9] allowing to outperform conventional confocal microscopy. The intensification of the local electromagnetic field originated from subwavelength confinement of light could be also exploited in Raman spectroscopy. However, to date this opportunity is still quite undeveloped. Yi *et al.* first observed that the Raman signal of a single-crystal Si substrate can be significantly increased when micron-sized SiO_2 spheres, acting as secondary lenses, are drop-casted over its surface.[10] Although useful to demonstrate the potential of the micro-lenses, Si single crystals are commonly used as spectral calibration standards and do not represent a real issue for Raman spectroscopy. From this point of view, the enhancement of Raman intensity obtained by combining a low numerical aperture (N.A.) objective with colloidal μ-lenses can be easily reached or even overcome simply by using a higher N.A. objective, so that bulk Si substrates do not allow to fully exploit the unique advantages offered by μ-lenses in term of spatial confinement of light.

In this paper SiO_2 microspheres are tested as μ-lenses for detecting thin films and molecular species under different

optical configurations, in order to explore their potential and limitations in more challenging contexts. Their performances are also compared to those of metal-based conventional SERS substrates. However, nanofocusing is not the only way for dielectric spheres to enhance Raman scattering. Mie-type resonances from either individual spheres or colloidal crystal assemblies can also be exploited,[11-13] and we have recently demonstrated that evanescent fields originating from whispering gallery mode resonances can allow for carrying out Raman analysis under non-perturbing conditions.[14] However, in these cases light confinement is maximized when the refractive index contrast between the dielectric sphere and background is > 2:1 and the spheres can work as optical cavities rather than lenses. In the last part of this paper we will demonstrate that μ-lenses can be synergistically coupled to core/shell colloidal crystal resonators (optical cavities) and, in general, to any kind of Raman-active substrates to enhance their overall sensitivity, playing as universal, disposable tools for Raman microspectroscopy.

Materials and Methods

SiO_2 microspheres: Commercial monodisperse SiO_2 microspheres (Microparticle-GmbH, size: 2.06 ±0.05 μm, 50 mg/mL) were used utilized as colloidal micro-lenses, by directly dropping 1 μL of either water of ethanol solution (dilution: 1/1000) on the surface of the target. Further details on individual experiments are given in Results and Discussion section.

MicroRaman analysis: The Raman measurements were carried out by means of a high-resolution Raman microscope (Labram HR-800, Horiba/Jobin-Yvon. Exciting source: He-Ne laser (λ=633 nm), with different numerical aperture objectives (0.50, 0.75, 0.9) in backscattering configuration. A scheme of each individual experimental configuration is given in the Results and Discussion section. All data reported in Figure 1, 2 and 3 b results from sampling over 30 different spheres. Each spectrum results from the average of three measurements and is automatically generated by the acquisition software (LabSpec). Error bars indicate the standard deviation.

The analysis of thin and ultra-thin films was carried out on TiO_2 layers deposited onto Si (100) single-crystal wafer by atomic layer deposition (ALD), through the same procedure described in ref. 13. The thickness of the samples was controlled by changing the number of ALD cycles and checked by x-ray reflectivity (XRR) measurements. 5, 25, 50 and 100 nm-thick films were selected for Raman experiments. The as deposited samples were annealed in air at 700°C for 4 h to produce fully crystalline anatase films.

Different Methylene Blue (MB, $C_{16}H_{18}N_3SCl$, Sigma-Aldrich) solutions (concentration range: 10^{-3}-10^{-9} M, pH: 6.9) were used to test the capabilities of micro-lenses in detection of molecular probes. A comparison to conventional, metal-based SERS substrates was carried out by coating a reference Si substrate with an ultra-thin (nominal thickness: 3 nm) layer of Au nanoislands, deposited by a K550 sputtering coater (discharge current: 25 mA, total pressure: 10^{-1} mbar, room temperature). SiO_2/TiO_2/core/shell microspheres (T-rex) were used as an example of non-conventional, metal-free SERS active substrates. The preparation of T-rex is described in ref. 13. The experiments reported in this paper were carried out on T-rex20 samples, consisting of SiO_2 cores (size: 2 μm) coated with a 20 nm-thick layer of anatase. Three dimensional assemblies of T-rex were used as core/shell colloidal crystals to infiltrate and analyse biomolecules in solution. Here the application of μ-lenses for Raman detection of biomolecules under real working conditions was tested with 1mM water solution of glutathione (L-γ-glutamyl-cysteinyl-glicine, GSH, Sigma-Aldrich).

Results and discussion

The effects of SiO_2 colloidal μ-lenses on Raman response were investigated in different experiments. Amorphous SiO_2 spheres were chosen as dielectric lenses because they do not have any Raman signals that can interfere with those of the analytes. In addition, charge transfer transitions between SiO_2 and analytes can be ruled out (E SiO_2 conduction band: -0.95 eV, E SiO_2 valence band: -9 eV). A detailed description of the theoretical background related to photonic nanojet can be found in literature.[1-7] On the basis of the model described in reference 3 we can assume that the lateral size of a photonic nanojet propagating from 2 μm-sized silica spheres excited at λ=633 nm is □240 nm (it is related to the wavelength of the incident light as 0.375λ). The first series of microRaman experiments was focused on the analysis of TiO_2 thin films with thicknesses ranging from 5 to 100 nm. These experiments enabled us to test the relative amplification of the Raman intensity as a function of the optical setup and demonstrate that this approach can remarkably extend the limit of detection of continuous layers. Our investigation was then carried on through the detection of molecules in solution, using different concentrations of MB as a molecular probe. Here the analytical capabilities of the μ-lenses were compared to those of conventional, SERS-active gold nanoparticles. We also demonstrated that μ-lenses and metal nanoparticles can be synergistically coupled to further extend the performances of SERS substrates. Finally, different proof-of-concept experiments were carried out in order to combine μ-lenses with core/shell colloidal crystals, which have been recently exploited to monitor chemical reactions under real working conditions.

Analysis of thin films

The effect of μ-lenses was tested by acquiring the Raman spectra of uniform anatase thin films with four different thicknesses (5, 25, 50 and 100 nm) deposited onto Si single crystal wafers. Colloidal monodisperse SiO_2 microspheres (size: 2±0.05 μm) were spread over the thin film surface from a

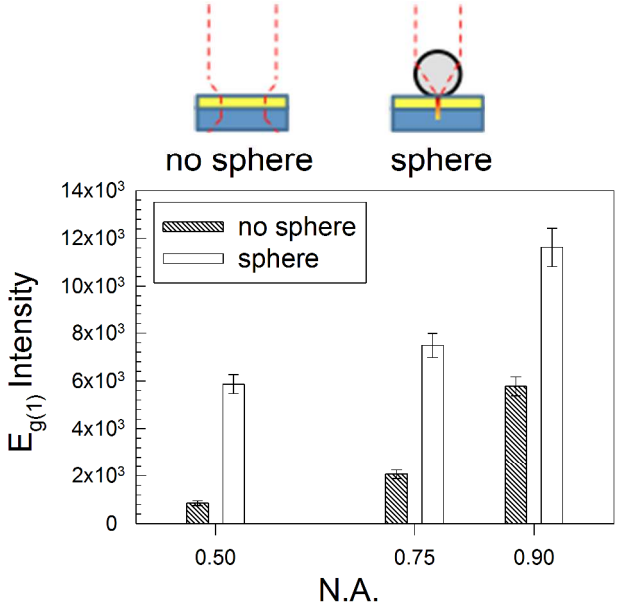

Figure 1. Analysis of Raman spectra (anatase $E_{g(1)}$ mode) collected from 30 individual SiO_2 μ-lenses (acquisition time: 20s) as a function of the objective numerical aperture, compared to the same planar thin films without spheres.

diluted solution (*see* Experimental Section). The exciting laser was focused on the top of the surface of individual spheres and Raman spectra were acquired in backscattering geometry. Reference spectra of the thin films were acquired from different regions of the same sample in the absence of μ-lenses (*see* SI 1). The uniformity of ALD coatings ensures that the thickness of the anatase layer is the same all over the sample. The first series of measurements were carried out using microscope objectives with numerical apertures (N.A.) ranging from 0.50 to 0.90, in order to test the performances of μ-lenses under different conditions of light collection. The intensity of the anatase main peak ($E_{g(1)}$ mode) was evaluated for planar thin films (thickness: 100 nm) with and without μ-lenses. Figure 1 shows the results of Raman spectra collected from thirty spheres compared to those of different regions of the planar thin film deposited onto the same Si substrate. In all of the cases μ-lenses allow the intensity of the anatase peak to be significantly enhanced, indicating that light is efficiently focused through the spheres and the Raman response of the underlying film can take advantage of such a local increase of the electromagnetic field.

Higher N.A. objectives limit the penetration of the incident light and extend the angle of collection of the backscattered radiation, so that the spectral intensity is related to the choice of the microscope objective and, as expected, the maximum absolute value in Raman intensity was obtained for spheres irradiated through the higher N.A. objective (0.90). However, there are two interesting points to highlight. First, for all the objectives used in these measurements the intensity obtained from μ-lenses is higher than that achievable from planar thin films (*i.e.* without lenses) analyzed through a higher N.A. objective. For example, the Raman intensity resulting from lenses irradiated through a 0.50 N.A. objective is higher than that achievable using a 0.75 N.A. and comparable to that of a 0.90 N.A. objective without lenses. A similar trend was found for the 0.75 N.A. objective. These data indicate that μ-lenses and their effects on the enhancement of spectral intensity of a thin layer are significantly stronger than those achievable by conventional microspectroscopy and cannot be compensated by simple switching from lower to higher N.A. objectives. It should also be observed that the strongest enhancement in the relative intensity ratio between sphere-coated and reference films is achieved by the lowest N.A. objective. This result is in qualitative agreement with the experiments reported by Yi *et al.* on bulk silicon.[10] In that paper the authors found that the maximum enhancement of the Raman intensity between sphere-coated and uncoated bulk Si substrates (ERI) is about 6. This value is achieved when the size of the sphere approaches that of the incident laser beam waist (□2.5 μm). On the basis of geometrical considerations they also calculated that the Raman enhancement factor (EF) achievable using SiO_2 spheres with an optimal size of 2.5 μm is around 10^4. In our case, a direct comparison of ERI between the main Raman modes of anatase ($E_{g(1)}$) and Si (TO) in anatase-coated Si substrates enabled us to elicit the specific sensitivity of μ-lenses to the analysis of thin layers, unravelling that using a 0.5 N.A. objective the relative enhancement of Raman intensity of the anatase mode is remarkably stronger (□7 vs. 4) than that of the underlying Si substrate. (SI 2) This enhanced sensitivity might be explained considering that photons coming from the Si substrate are gathered more efficiently as the solid angle of light collection is increased using higher N.A. objectives. As a result, the sensitivity towards the thin film is strongly reduced. Moreover, higher N.A. aperture objectives are more sensitive to the position of the focal point on the sphere, as demonstrated by the increase of error bars on passing from 0.5 to 0.9 N.A. objectives. For all of these reasons, and since μ -lenses could find interesting applications in microfluidic chambers and operando-like reactors, where 0.5 N.A. long-working distance objectives represent a suitable solution for acquiring Raman spectra, all of the following experiments were carried out with 0.5 N.A. objectives.

Figure 2 shows the results of measurements on anatase layers as a function of the film thickness with or without addition of colloidal μ-lenses over thirty different regions. These data show that μ-lenses allow for a general enhancement of Raman scattering. The maximum ERI is achieved for thicker films (100 nm), indicating that under these conditions the nanojet beam propagates across the coating layer for more than 50 nm before being focused. However, although their absolute intensity is quite low, the Raman signals of the thinnest (20 and 5 nm-thick) anatase layers were detected only by means of μ-lenses.

These data show that even ultra-thin layers can significantly experience the beneficial effects of field enhancement induced by μ-lenses. This allows for extending the detection limit to a thickness level that cannot be usually reached by conventional microRaman. Moreover, colloidal microspheres can be quickly

dispersed on a thin film surface, used as μ-lenses for the Raman analysis and then easily removed by sonication. This three-step procedure allows for probing and investigating thin layers through a non-destructive approach that does not alter the original structure of the film.

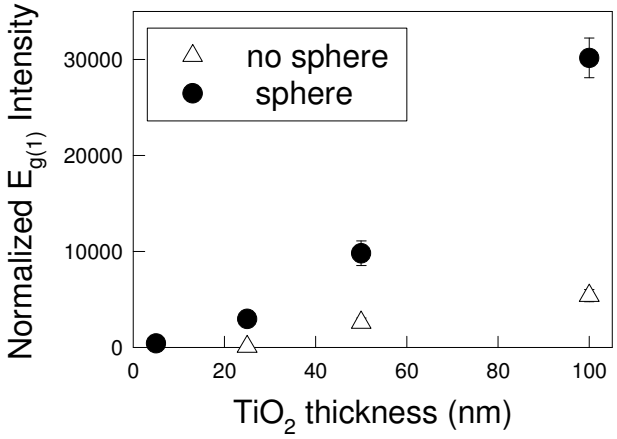

Figure 2. Normalized intensity of the anatase $E_{g(1)}$ Raman mode as a function of film thickness. Spectra were acquired over 30 different areas with or without single SiO_2 spheres using a 0.50 N.A. microscope objective. If not indicated, error bars are included within the experimental point size.

Analysis of molecular species and comparison to metal-based SERS substrates

The potential of μ-lenses in detection of molecular species was tested using MB solutions over a wide concentration range (from 10^{-3} to 10^{-9} M). The Si substrates were soaked in a vessel containing 4 mL of dye solution. Upon drying at room temperature, each sample was analyzed by measuring different regions of the substrate. All the selected areas were flat and clean; optically visible agglomerates of MB were not considered in sampling (see SI 3). As a selected example, Figure 3a shows the Raman spectra of a 10^{-3} M MB solution acquired with and without colloidal μ-lenses using a 0.50 N.A. objective. The results of measurements extended over the whole concentration range is shown in Figure 3b, which refers to the intensity of the MB main peak around 1625 cm^{-1} (C-C ring stretching mode). Again, μ-lenses strongly enhance the MB Raman signal (the intensity ratio between the peak of a 10^{-3} M solution analyzed with and without μ-lenses is about 30) and extend sensitivity to very low concentration (10^{-7} M), *i.e.* three orders of magnitude beyond the detection limit of the analogous planar reference.

It is now interesting to compare the enhanced Raman scattering achieved by μ-lenses to that resulting from more conventional, metal-based SERS substrates. In general SERS-active materials consist of Ag or Au nanoparticles that are deposited from solution giving rise to fractal-like aggregates.[15] These aggregates are characterized by a dense distribution of SERS "hot-spots", which originate from junctions between two or more individual NPs. Hot-spots can allow to reach the ultimate detection limits of this technique (*e.g,* in single molecule detection experiments). However, the intensity of the enhancement strongly depends on hot-spots distribution, which is very hard to predict. In order to obtain a more homogeneous signal we prepared our SERS active substrates through a sputter-coating deposition of Au nanoislands onto the surface of a Si wafer.[16,17] Although not optimized for achieving the strongest SERS effects (the limit of detection of MB is only 10^{-8} M for sputter-coated substrates, just one order of magnitude lower than that obtained by μ-lenses without gold), this approach gives much more reproducible results than fractal assemblies, allowing to test μ-lenses under reliable conditions. (SI 4) Figure 4a shows as an example the C-C ring stretching Raman mode at 1625 cm^{-1} of a 10^{-5} M MB solution adsorbed onto Au nanoisland thin films and the same area upon focusing through SiO_2 μ-lenses. As predicted by finite-difference time-domain (FDTD) simulations, a metal layer is expected to reduce the penetration depth of a nanojet, leading to a more effective confinement of light at the SiO_2/metal interface.[18,19] Colloidal lenses enhance the intensity by a □ 1.5 factor. As reported in the inset of Figure 4a, μ-lenses extend the limit of detection to less than 10^{-9} M, *i.e.* one order of magnitude lower than that of Au nanoislands without lenses. Figure 4b summarizes the results of MB detection using different substrates. Colloidal lens-assisted detection on Au nanoislands outperforms the sensitivity of simple planar substrates by 5 orders of magnitude and even stronger effects can be expected by using more efficient metal-based SERS substrates.

These results indicate that the use of colloidal lenses is a convenient and very practical means to extend the Raman sensitivity of any type of SERS active substrate when the analyte is uniformly distributed all over the substrate itself. On the other hand, the main concern about the use of μ-lenses for analysis of molecular probes or inhomogenous samples is related to their positioning. Spontaneous self–assembly makes no possible to control the position of the lenses *a priori*. The functionalization of the lenses with functional groups that selectively bind to analytes could be possible (for example silica beads can be easily terminate with amine, thiol or carboxylic groups) but this would make the lens approach limited to the detection of specific analytes and, definitely, more complicated. Use of micromanipulators represents a fully mechanical alternative for positioning of lenses with micron-sized precision (an example of lens positioning is reported in SI 5). However, this obviously implies the introduction of an additional component into the analytical system. Optical gradients might be a further option to drive the positioning of lenses directly through the optical microscope used for microRaman analysis, but additional experiments are needed to explore this option in a more systematic way.

Another potential drawback related to the analysis of molecular probes could be related to the solvent used for the microspheres suspensions (in general water or ethanol).

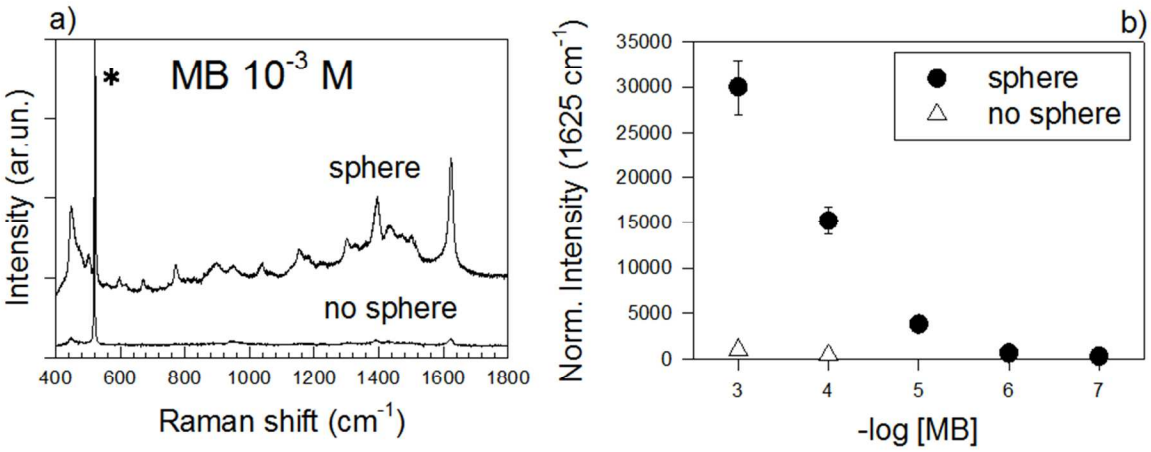

Figure 3. a) Example of Raman spectra of a MB solution (concentration: 10^{-3}M) drop-casted onto Si substrates and acquired through a 0.50 N.A. microscope objective with or without SiO_2 colloidal micro-lenses (see the main text for details). The Si peak of the substrate is indicated by an asterisk; b) Normalized intensity of the 1625 cm^{-1} MB peak (corresponding to the C-C ring stretching mode) as a function of MB concentration. Spectra were acquired over 30 different areas with or without single SiO_2 spheres, using a 0.50 N.A. microscope objective. If not indicated, error bars are included within the experimental point size.

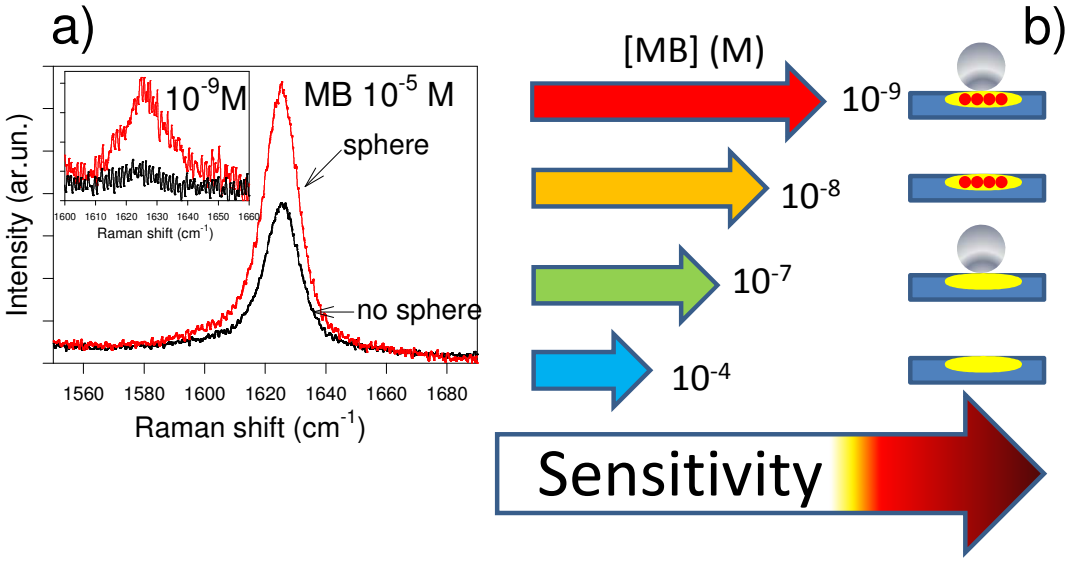

Figure 4. a) Example of SERS spectra of a 10^{-5} M MB solution adsorbed onto Au nanoisland substrates either in the presence or absence of SiO_2 microspheres acting as colloidal micro-lenses. Micro-lenses allow to extend the Raman sensitivity of metal-based SERS substrates in MB detection below 10^{-9} M, as shown in the inset; b) Schematic summary showing the progressive increase of detection capability as a function of the optical configuration (planar Si, spheres, SERS substrate and spheres+ SERS substrate).

When the microspheres are spread over the analyte, they could dissolve it. However, as demonstrated by the results on MB, in general this is not a critical issue, because the solution is re-dried on the substrate before measuring. If the microspheres were directly mixed to the analyte solution, part of the analyte could be directly adsorbed at their surface upon deposition. As reported by Anderson,[11] this would allow for the exploitation of additional enhancement effects due to evanescent fields originated from whispering gallery modes, as well as pre-concentration resulting from adsorption. However, this option may open further issues about reproducibility, which is strongly affected by inhomogeneous adsorption of the analyte. A detailed investigation of these aspects is beyond the scope of this paper, which is restricted to the evaluation of μ-lens effect, and will be the object of future research activity.

Comparison and coupling to core/shell colloidal crystal traps

As we have demonstrated in a previous paper,[13] core/shell beads characterized by a strong refractive index contrast between inner spherical cores and outer shell layers (*e.g.* SiO_2/TiO_2 core/shell, the so-called T-rex colloids) give rise to enhanced Raman scattering because of the synergistic combination of both intra- and inter-colloid multiple reflections and morphology-dependent Mie resonances. Figure 5a shows the Raman spectra of a 20-nm thick anatase layer deposited either on planar Si or SiO_2 microspheres (T-rex 20). As we have already observed in previous experiments, the anatase modes of such a thin layer cannot be detected without using μ-lenses. However, the intensity of the Raman signal obtained by μ-lens focusing is remarkably lower (less than a half) than that obtained by T-rex substrates. These results point out that μ-lens focusing cannot reach the same efficiency of light trapping and total internal reflection in production of Raman photons. Light trapping and confinement can be directly monitored by observing the intensity of the main peak (TO) of the Si substrate (Figure 5b). A clear inverse correlation between Si and TiO_2 signals is observed. The 20 nm anatase layer is enough to significantly reduce the penetration of the exciting light induced by μ-lens overfocusing. As a consequence, SiO_2 μ-lenses can be converted into core/shell light traps by coating silica with higher refractive index layers (*e.g.* TiO_2). In this case, part of the original, non-evanescent field is transformed into evanescent waves originating by total internal reflections. These results agree with Poynting vector field simulations based on Mie theory, (as well as on FDTD) which have been reported in literature for colloidal spheres with different refractive indexes.[19] Even more interesting results are observed when the SiO_2 μ-lenses are deposited onto a monolayer of SiO_2/TiO_2 core/shell beads (lens-on-T-rex). This configuration allows for a remarkable enhancement (three times more intense) of the Raman signal of the TiO_2 shell layer, which corresponds to the complete extinction of the Si peak. These data suggest that the μ-lens focuses the incident light into the T-rex bead, and the latter behaves as an efficient optical cavity. It is important to note that, in the absence of μ-lenses, the Si signal disappears (*i.e.* light is fully trapped) only when more than four layers of T-rex20 beads are stacked in colloidal assemblies.[13] Thus, μ-lenses allow to boost the self-diagnosis capability of Raman-active colloidal resonators. The origin of this effect deserves further investigation, however we might hypothesize that μ-lens focusing can be more efficient in exciting morphology-dependent resonances[20,22](*e.g.* whispering gallery modes) within the titania layer of a T-rex.

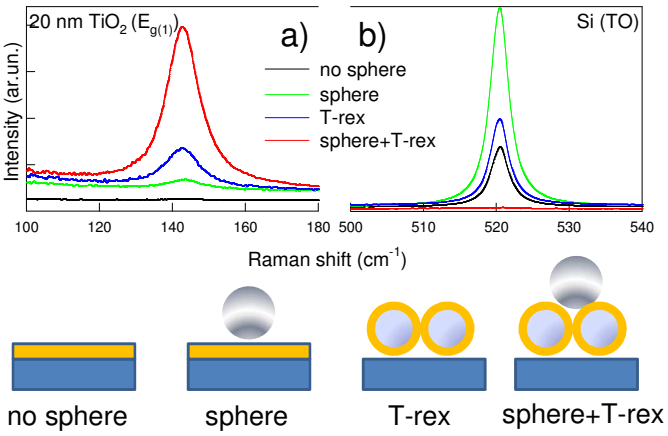

Figure 5. Raman spectra of a 20 nm-thick anatase layer acquired under different optical configurations: a) anatase $E_{g(1)}$ mode (N.A. objective: 0.50. Acquisition time: 20 s); b) Si substrate (TO mode) (N.A. objective: 0.50. Acquisition time: 5 s.) All the different experimental configurations (no sphere, sphere, T-rex and sphere+T-rex) are schematically represented below (*see* the main text for further details).

We have also tested the combination of μ-lenses and core/shell Raman resonators in a different configuration. In a recent paper we have shown that core/shell colloidal crystals can be exploited to detect biological probes and their reactions in aqueous environment.[14] The analyte solution is entrapped within the colloidal crystal and can take full advantage of multiple light scattering events occurring between close packed spheres upon laser excitation. In the present case we carried out the same experiment of glutathione (GSH) detection described in our previous paper with the addition of SiO_2 μ-lenses (*see* scheme in Figure 6). Briefly, a T-rex based colloidal crystals was infiltrated with 1mM solution of GSH. Upon drying, the exceeding solution forms a viscous thin film on the surface of the colloidal crystal. The μ-lenses were deposited onto this layer and the Raman spectra were acquired using a long-working distance 50x objective (N.A.: 0.50). Figure 7 shows the results of GSH detection with and without μ-lenses. The Raman signal was increased by a factor of □ 2 in the presence of μ-lenses. The Raman detection of GSH from aqueous solution represents a direct test-bench to evaluate the perturbation introduced by μ-lens focusing on the molecular structure. The position of the Raman bands related to the

stretching vibrations of both –SH group of the cysteinyl residue (at □ 2565 cm^{-1}) and $–CH_2$- molecular backbone are identical to those of the molecule in solution, indicating that the GSH structure in viscous thin film is not significantly affected by μ-lens focusing, in spite of its non evanescent nature. This could be related to the presence of the aqueous environment, which strongly attenuates heating effects, and deserves further investigation. Taking all these experimental observation into account we could argue that in this configuration the colloidal μ-lens play as amplifiers for backscattered Raman radiation, allowing to maintain the unique advantages offered by T-rex substrates in terms of low invasiveness. This feature makes μ-lenses powerful tools to complement and improve the performances of T-rex in detecting molecular species and chemical reactions under real working conditions.[14]

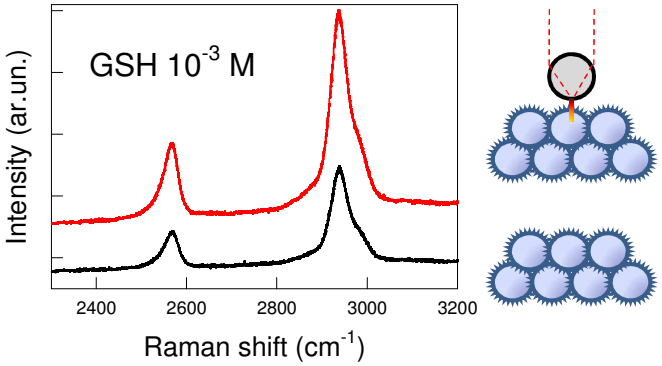

Figure 6. Raman spectra of a 10^{-3} M GSH solution infiltrated into a T-rex core/shell colloidal crystals with and without addition of SiO_2 μ-lenses.

Conclusions

Our experiments demonstrate that colloidal μ-lenses can be used as universal tools to enhance Raman scattering. They have been tested in detection of ultra-thin films and molecular species. The contribution of a μ-lens to Raman response is strongly dependent on both the type of analyte under investigation and optical setup (*e.g.* use of microscope objective with different N.A. in backscattering measurements). These two factors affect the penetration depth of the photonic jet emerging from the μ-lens. As a consequence, the spatial confinement of the exciting light and the resulting near-field enhancement are strongly related to the macro-lens/μ-lens/analyte setup and can be finely tuned. In parallel, depending on their structure and polarizability, different analytes exhibit different sensitivity to the enhanced local field. However, as a general trend, μ-lenses provide a systematic enhancement of Raman scattering that outperforms that achievable by conventional Raman microspectroscopy. This represents a crucial benefit in analysis of thin films. Our experimental data demonstrate that μ-lenses can boost the sensitivity of a Raman measurement, allowing to detect layers of few nanometers. Here μ-lenses offer unique advantages because they can be easily placed on any kind of coated surface by drop-casting from a solution and easily removed after the measurement. Micro-manipulators could also be used when more precise spatial localization of the μ-lenses is needed. Thus, μ-lenses can be exploited as non-destructive, disposable tools for microRaman spectroscopy.

In the case of detection of molecular species, μ-lenses can be combined to conventional SERS substrates to achieve extra-sensitivity and extend detection limits. When coupled to core/shell colloids characterized by high contrast of refractive index between core and shell (*e.g.* T-rex), μ-lenses allow to promote an efficient excitation of morphology-dependent resonances. As a result, the advantages related to colloidal crystal traps can be further enhanced by this combination. The use of colloidal μ-lenses in microRaman spectroscopy can open exciting perspectives also in the analysis of chemical reactions under real working conditions,[23-25] with particular regard to biological systems (*e.g.* cellular membranes and extracellular vesicles) where, in addition to Raman scattering, the confinement of light induced by μ-lenses can be synergistically exploited to obtain enhanced fluorescence and imaging.[26-28]

Acknowledgements

We thank Dr. Marco Salmistraro for support in preparation of anatase thin films and Prof. Matteo Ferroni for micromanipulation experiments. This work was partially supported by SUPRANANO (INSTM-Regione Lombardia project).

Notes and references

[a] INSTM and Chemistry for Technologies Lab., University of Brescia, via Branze 38, 25123 Brescia (ITALY). E-mail: ivano.alessandri@unibs.it

Electronic Supplementary Information (ESI) available Optical microscope images of SiO_2 microspheres deposited onto TiO_2 thin films and MB adsorbates. Comparison between ERI of anatase layer (thickness:100 nm) and Si substrate as a function of N.A. Optical and SEM characterization of Au nanoislands. Examples of sampling procedure and micromanipulation.

1. Z. Chen, A. Taflove, V. Backman, *Opt. Express*, 2004, **12**, 1214-1220.
2. S. Lecler, Y. Takakura, P. Meyreuis, *Opt. Lett*. 2005, **30**, 2641-2643.
3. A. Heifetz, S-C. Kong, A. V. Sahakin, A. Taflove, V. Backman, *J. Comput. Theor. Nanosci.* 2009, **6**, 1979-1992.
4. A. Heifetz, J. J. Simpson, S-C. Kong, A. Taflove, V. Backman, *Opt. Express* 2007, **15**, 17334-17342.
5. S. Lecler, S. Haacke, N. Lecong, O. Crégut, J-L. Rehspringer, C. Hirlimann, *Opt. Express* 2007, **15**, 4935-4942.
6. D. Gérard, J. Wenger, A. Devilez, D. Gachet, B. Stout, N. Bonod, E. Popov, H. Rigneault, *Opt. Express* 2008, **16**, 15297-15303.
7. A. Devilez, N. Bonod, B. Stout, D. Gérard, J. Wenger, H. Rigneault, E. Popov, *Opt. Express* 2009, **17**, 2089-2094.
8. J. J. Schwartz, S. Stavrakis, S. R. Quake, *Nature Nanotechnol*. 2010, **5**, 127-132.

9. H. Yang, M.A. Gijs, *Anal. Chem.* 2013, **85**, 2064-2071.
10. K. J. Yi, H. Wang, Y. F. Lu, Z. Y. Yang, *J. Appl. Phys*. 2007, **101**, 063528.
11. D. Christie, J. Lombardi, I. Kretzchmar, *J. Phys. Chem. C*. 2014, **118**, 9114-9118.
12. M. S. Anderson, *Appl. Phys. Lett*. 2010, **97**, 131116.
13. I. Alessandri, *J. Am. Chem. Soc*. 2013, **135**, 5541-5544.
14. I. Alessandri, L. E. Depero, *Small* 2014, **10**, 1294-1298.
15. E. C. Le Ru, P.G. Etchegoin, *Principles of Surface-Enhanced Raman Spectroscopy*, Elsevier, Amsterdam, 2009.
16. A. Merlen, V. Gadenne, J. Romann, V. Chevallier, L. Patrone, J. C. Valmalette, *Nanotechnology* 2009, **20**, 21570
17. G. Sinha, L.E. Depero, I. Alessandri, *ACS-Appl. Mater. Interfaces* 2011, **3**, 2557-2563.
18. J. F. Cardenas, *J. Raman Spectrosc*. 2013, **44**, 540-543.
19. S. Lee, L. Li, Z. Wang, *J. Opt.* 2014, **16**, 015704.
20. L. K. Ausman, G. C. Schatz, *J. Chem. Phys*. 2008, **129**, 054704.
21. Z. B. Wang, B. S. Luk'yanchuk, M. H. Hong, Y. Lin, T. C. Chong, *Phys. Rev. B*. 2004, **70**, 035418.
22. D. J. Norris, M. Kuwata-Gonokami, W. E. Moerner, *Appl. Phys. Lett*. 1997, **71**, 297-299.
23. M. Salmistraro, A. Schwartzberg, W. Bao, L. E. Depero, A. Weber-Bargioni, S. Cabrini, I. Alessandri, *Small* 2013, **9**, 3301-3307.
24. A. Yashchenok, A. Masic, D. Gorin, B. S. Shim, N. Kotov, P. Frantzl, A. G. Möhwald, Skirtach, *Small* 2013, **9**, 351-356.
25. N. M. Dimitrijevic, E. Rozhkova, T. Rajh, *J. Am. Chem. Soc.* 2009, **131**, 2893-2899.
26. K. A. Antonio, Z. D. Schultz, *Anal. Chem*. 2014 **86**, 30-46.
27. Z. Ali, A. Z. Abbasi, F. Zhang, P. Arosio, A. Lascialfari, M. F. Casula, A. Wenk, W. Kreyling, R. Plapper, M. Seidel, R. Niessner, J. Knoll, A. Seubert, W. J. Parak, *Anal. Chem*. 2011, **83**, 2877-2882.
28. S. Carregal-Romero, E. Caballero-Diaz, L. Beqa, A. M. Abdelmonen, M. Ochs, D. Huhn, B.S. Suau, M. Valcarcel, W. J. Parak, *Ann. Rev. Anal. Chem.* 2013, **6**, 53-51.

